Shape coexistence in ^{187}Au

J. K. Johansson, D. G. Popescu,* D. D. Rajnauth, and J. C. Waddington
Tandem Accelerator Laboratory, McMaster University, Hamilton, Canada L8S 4K1

M. P. Carpenter,† L. H. Courtney, V. P. Janzen,‡ A. J. Larabee,§
Z. M. Liu,** and L. L. Riedinger
Department of Physics, University of Tennessee, Knoxville, Tennessee 37996
(Received 16 January 1989)

The level structure of odd-proton ^{187}Au was studied using the ^{172}Yb(^{19}F,4n) reaction. Gamma-gamma coincidence, angular distributions and γ-γ-time measurements were used to establish the energies, spins, parities, and lifetimes for the states in the decay scheme of ^{187}Au. Both prolate and oblate structures have been established. The prolate bands are built on the $\pi h_{9/2}$ ($\alpha=\pm\frac{1}{2}$) and the $\pi i_{13/2}$ ($\alpha=\frac{1}{2}$) particle states. An oblate, strongly coupled band built on a 90±10 ns isomeric state is reported for the first time. A second oblate structure built on the $h_{11/2}$ proton-hole state was established to much higher spin than before. The backbend present in the $\pi i_{13/2}$ band has been interpreted as the alignment of a pair of $h_{9/2}$ protons.

I. INTRODUCTION

There is a well-known region of shape coexistence in the Pt-Au-Hg nuclei. The low-lying 0^+, 2^+ states in the Hg isotopes are thought to have an oblate shape while the second 0^+, 2^+ states decrease rapidly in excitation energy from ^{188}Hg to ^{184}Hg and have been described as having prolate shapes.[1-5] The opposite is true in the light Pt isotopes. Whereas the ground state properties of heavy Pt isotopes ($N=110-116$) are similar to those of the Hg nuclei, the lowest 0^+ states in $^{178-186}$Pt are prolate with the excited states being oblate. The gold nuclei have the same shape coexistence.[6,7] The $\pi h_{11/2}$ system remains fairly constant in energy, while the $\pi h_{9/2}$ and $\pi i_{13/2}$ decrease very rapidly as one goes away from the $N=128$ closed shell. The $h_{11/2}$ excitations are thought to result from proton-hole states coupled to even-even Hg cores while the $h_{9/2}$ and $i_{13/2}$ excitations are proton particle states coupled to even-even Pt cores.

In ^{185}Au, bands built on the $\pi h_{9/2}$, $\pi i_{13/2}$, and $\pi f_{7/2}$ states have been identified as prolate and the $\pi h_{11/2}$ structure as oblate.[8] The oblate structures are expected to be more prominent in $N=108$ ^{187}Au which has ^{186}Pt and ^{188}Hg cores. Since these core nuclei are well studied,[9-11] the ^{187}Au case should provide an excellent probe of the shape driving effects of the odd nucleon.

Previous to this study little was known about the nuclear structure of high-spin states in ^{187}Au. Bands built on the $\pi h_{11/2}$, $\pi h_{9/2}$, and $\pi i_{13/2}$ Nilsson states were found in this study. The $\pi h_{9/2}$ band has been extended beyond the previous known members.[6,7] The $\pi i_{13/2}$ band was seen for the first time. An irregular sequence of levels based on the $\pi h_{11/2}$-hole state was seen much higher in spin than before and a strongly coupled band built on an isomeric state ($T_{1/2}=90\pm10$ ns) was established which decays to both the $h_{9/2}$ and $h_{11/2}$ bands. In addition, two other isomers were found with $T_{1/2}$ of 25±3 and 50±5 ns.

II. EXPERIMENTAL METHODS

Beams from the McMaster University FN Tandem Accelerator were used to populate the high-spin states of ^{187}Au with the ^{172}Yb(^{19}F,4n) reaction. The isotopically enriched ^{172}Yb (98%) target was bombarded with the 95-MeV ^{19}F beam. The target was 2.0 mg/cm^2 thick and backed with 5.3 mg/cm^2 of ^{208}Pb.

A multiplicity filter consisting of two 12.7 cm×15.2 cm and four 7.6 cm×7.6 cm NaI scintillation counters, was used to enhance the detection of high-spin transitions and to discriminate against the nonreaction events. The NaI detector faces were covered with Pb, Cd, and Cu shields to reduce the intensity of the Pb x rays. In addition, the four 7.6 cm×7.6 cm NaI counters around the beam tube were shielded from each other with Pb to prevent scattering from one detector to another.

An array of five coaxial Ge detectors was mounted at angles of roughly 90, 60, 45, 30 and −10° to the beam direction at 9–10 cm distances from the target. The accepted events consisted of at least three Ge detectors firing or at least two Ge and two NaI detectors firing. The amplifier gains of the five Ge detectors were matched so that coincidences in any two detectors could be considered. An additional planar Ge detector was placed at −90° for detecting the low-energy γ rays with good energy and time resolution in order to measure lifetimes in the nanosecond range. A subsequent angular distribution experiment used a similar Ge (coaxial) detector arrangement.

The data were sorted off line into a symmetric 1024×1024 channel coincidence matrix and the background was subtracted with the method of Palameta and Waddington.[12] The background under the discrete lines which results mostly from continuum γ rays and Compton distributions was successfully subtracted by this means. After correcting the subtracted matrix for detector efficiency, final gated γ-γ coincidence spectra were obtained for analysis.

III. RESULTS

Prior to this investigation, several of the high-spin states in ^{187}Au had been studied by various groups.[6,7] The level scheme of ^{187}Au constructed from the results of the present experiment is shown in Fig. 1. All of the gamma transitions in the level scheme above the $\frac{9}{2}^-$ state were assigned from the analysis of individual γ-γ coincidence spectra. Information concerning the gamma transitions consisting of γ-ray energies, intensities, angular distribution coefficients, and multipole assignments is summarized in Table I. A complete explanation of the construction of the level scheme is too lengthy to describe. Instead, several gated spectra have been chosen that show strong evidence for the placements of the γ-ray transitions and give an indication of the quality of the data.

A. Decay scheme

For $Z=79$ Au, the proton Fermi level lies above the $h_{11/2}$ and below the $h_{9/2}$ and $i_{13/2}$ proton shells. Three families of states have been observed in ^{187}Au and have been interpreted as originating from the proton shells mentioned above.

The spins and parities for the bandheads of bands 1 and 6 were firmly established as $\frac{9}{2}^-$ and $\frac{11}{2}^-$ by Deleplanque *et al.*[6] The bandhead of band 3 has been assigned as $\frac{13}{2}^+$ based on the results of our angular distribution measurements. This assignment is consistent with that of Bourgeois *et al.*[7] Similar $\frac{13}{2}^+$ bands have also been found in ^{181,183,185}Au isotopes.[8,13–15] Spin assignments for the rest of the bands were then based on the angular distribution results. In the following discussion, bands 1 and 2 are referred to as the two signatures

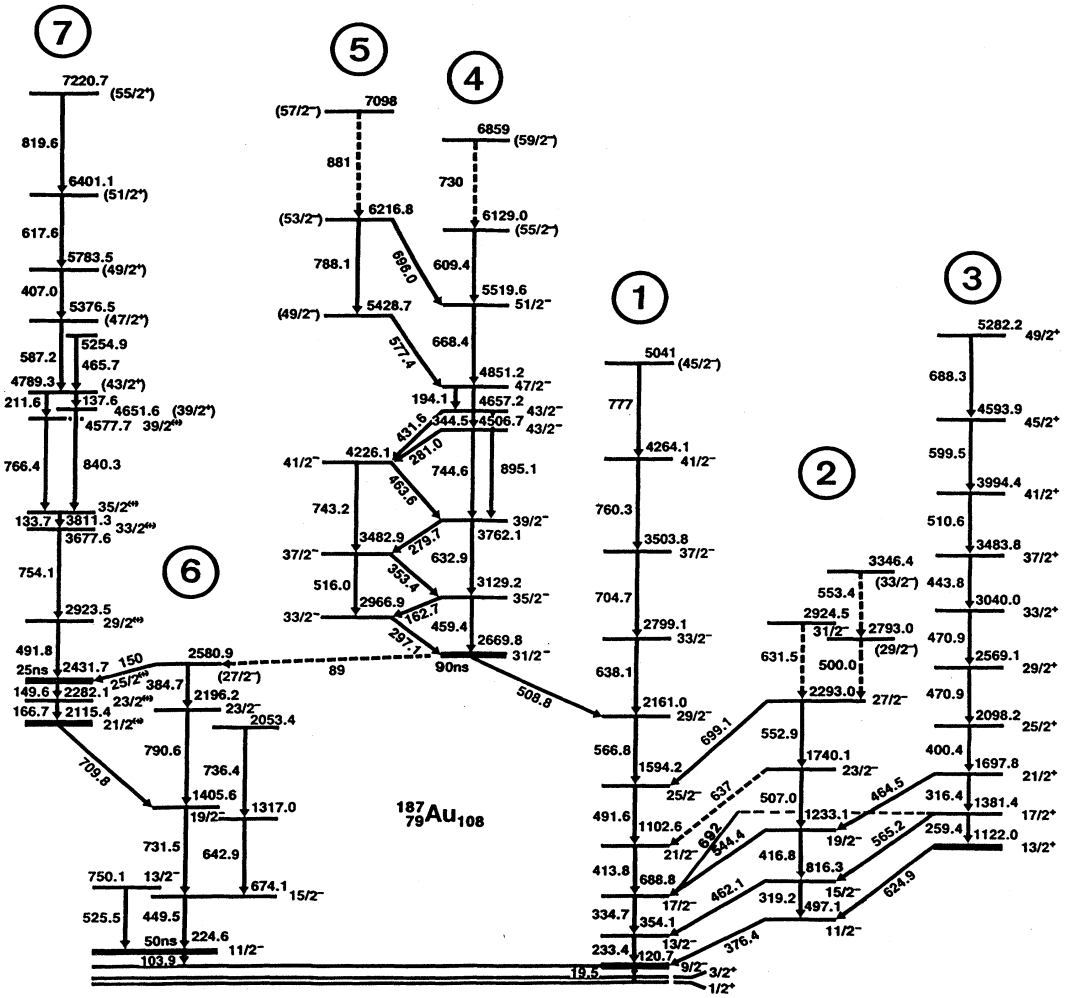

FIG. 1. Proposed level scheme for ^{187}Au based on the ^{172}Yb(^{19}F,4n) reaction. All transitions above the $\frac{9}{2}^-$ level were assigned from γ-γ coincidence spectra.

TABLE I. Transitions in ^{187}Au.

E_γ (keV)	I_γ[a]	A_2	A_4	$J_i^\pi \rightarrow J_f^\pi$	Multipolarity
89.0	2			$\frac{31}{2}^- \rightarrow \frac{27}{2}^-$	
103.9				$\frac{11}{2}^- \rightarrow \frac{9}{2}^-$	$M1/E2$
133.7	9	−0.12(4)	0.01(5)	$\frac{35}{2}^{(+)} \rightarrow \frac{33}{2}^{(+)}$	$M1/E2$
137.6	3			$(\frac{43}{2}^+ \rightarrow \frac{39}{2}^+)$	
149.6	17	−0.14(2)	−0.03(2)	$\frac{25}{2}^{(+)} \rightarrow \frac{23}{2}^{(+)}$	$M1/E2$
150				$(\frac{27}{2}^-) \rightarrow \frac{25}{2}^{(+)}$	
162.7	14	−0.33(3)	0.09(4)	$\frac{35}{2}^- \rightarrow \frac{33}{2}^-$	$M1/E2$
166.7	19	−0.14(2)	0.02(2)	$\frac{23}{2}^{(+)} \rightarrow \frac{21}{2}^{(+)}$	$M1/E2$
194.1	7			$\frac{47}{2}^- \rightarrow \frac{43}{2}^-$	
211.6	15	0.38(4)	−0.08(5)	$(\frac{43}{2}^+) \rightarrow \frac{39}{2}^+$	$E2$
233.4	=100	0.27(1)	−0.09(1)	$\frac{13}{2}^- \rightarrow \frac{9}{2}^-$	$E2$
259.4	4	0.07(4)	−0.08(5)	$\frac{17}{2}^+ \rightarrow \frac{13}{2}^+$	
279.7	23	−0.14(2)	0.07(2)	$\frac{39}{2}^- \rightarrow \frac{37}{2}^-$	$M1/E2$
281.0	3	−0.12(2)	0.09(2)	$\frac{43}{2}^- \rightarrow \frac{41}{2}^-$	$M1/E2$
297.1	43	−0.03(1)	0.09(1)	$\frac{33}{2}^- \rightarrow \frac{31}{2}^-$	$M1/E2$
316.4	29	0.28(1)	−0.10(2)	$\frac{21}{2}^+ \rightarrow \frac{17}{2}^+$	$E2$
319.2	7	0.39(3)	−0.12(3)	$\frac{15}{2}^- \rightarrow \frac{11}{2}^-$	$E2$
334.7	93	0.28(1)	−0.09(1)	$\frac{17}{2}^- \rightarrow \frac{13}{2}^-$	$E2$
344.5	8	0.19(6)	−0.06(8)	$\frac{47}{2}^- \rightarrow \frac{43}{2}^-$	$E2$
353.4	33	−0.15(2)	0.08(2)	$\frac{37}{2}^- \rightarrow \frac{35}{2}^-$	$M1$
376.4	11	−0.81(2)	0.19(2)	$\frac{11}{2}^- \rightarrow \frac{9}{2}^-$	$M1/E2$
384.7	5			$(\frac{27}{2}^-) \rightarrow \frac{23}{2}^-$	
400.4	27	0.30(1)	−0.10(2)	$\frac{25}{2}^+ \rightarrow \frac{21}{2}^+$	$E2$
407.0	6	−0.00(14)	−0.43(7)	$(\frac{49}{2}^+) \rightarrow (\frac{47}{2}^+)$	
413.8	81	0.26(1)	−0.07(1)	$\frac{21}{2}^- \rightarrow \frac{17}{2}^-$	$E2$
416.8	10	0.12(3)	−0.04(3)	$\frac{19}{2}^- \rightarrow \frac{15}{2}^-$	
431.6	2	−0.05(12)	0.45(15)	$\frac{43}{2}^- \rightarrow \frac{41}{2}^-$	$M1/E2$
443.8	19	0.38(3)	−0.16(4)	$\frac{37}{2}^+ \rightarrow \frac{33}{2}^+$	$E2$
449.5	64	0.25(1)	−0.11(1)	$\frac{15}{2}^- \rightarrow \frac{11}{2}^-$	$E2$
459.4	20	0.31(3)	−0.16(3)	$\frac{35}{2}^- \rightarrow \frac{31}{2}^-$	$E2$
462.1	4			$\frac{15}{2}^- \rightarrow \frac{13}{2}^-$	
463.6	7			$\frac{41}{2}^- \rightarrow \frac{39}{2}^-$	
464.5	14			$\frac{21}{2}^+ \rightarrow \frac{19}{2}^-$	
470.9	48	0.32(2)	−0.10(2)	$\frac{33}{2}^+ \rightarrow \frac{29}{2}^+$	$E2$
470.9				$\frac{29}{2}^+ \rightarrow \frac{25}{2}^+$	$E2$
491.6	71	0.31(1)	−0.15(1)	$\frac{25}{2}^- \rightarrow \frac{21}{2}^-$	$E2$
491.8	55			$\frac{29}{2}^{(+)} \rightarrow \frac{25}{2}^{(+)}$	
500.0	7	−0.23(4)	−0.05(5)	$\frac{29}{2}^- \rightarrow \frac{27}{2}^-$	$M1/E2$
507.0	8			$(\frac{23}{2}^- \rightarrow \frac{19}{2}^-)$	
508.8	48	−0.15(1)	0.04(2)	$\frac{31}{2}^- \rightarrow \frac{29}{2}^-$	$M1/E2$
510.6	16			$(\frac{41}{2}^+ \rightarrow \frac{37}{2}^+)$	
516.0	5			$\frac{37}{2}^- \rightarrow \frac{33}{2}^-$	
525.5		0.22(6)	0.05(7)	$\frac{13}{2}^- \rightarrow \frac{11}{2}^-$	
544.5	5	−1.10(7)	0.19(8)	$\frac{19}{2}^- \rightarrow \frac{17}{2}^-$	$M1/E2$

TABLE I. (*Continued*).

E_γ (keV)	I_γ[a]	A_2	A_4	$J_i^\pi \rightarrow J_f^\pi$	Multipolarity
553.1	14	0.05(4)	−0.02(5)	$(\frac{27}{2}^- \rightarrow \frac{23}{2}^-)$	
				$(\frac{33}{2}^- \rightarrow \frac{29}{2}^-)$	
565.2	13	−0.40(2)	0.18(3)	$\frac{17}{2}^+ \rightarrow \frac{15}{2}^-$	
566.8	64	0.30(1)	−0.10(1)	$\frac{29}{2}^- \rightarrow \frac{25}{2}^-$	$E2$
577.4	5	0.08(12)	0.03(15)	$(\frac{49}{2}^- \rightarrow \frac{47}{2}^-)$	$(M1/E2)$
587.2	16	0.36(6)	−0.22(7)	$(\frac{47}{2}^+ \rightarrow \frac{43}{2}^+)$	$E2$
599.5	10	0.70(5)	0.33(6)	$\frac{45}{2}^+ \rightarrow \frac{41}{2}^+$	
609.4	5	0.13(9)	0.49(12)	$(\frac{55}{2}^- \rightarrow \frac{51}{2}^-)$	
617.6	5	−0.15(9)	−0.33(11)	$(\frac{51}{2}^+ \rightarrow \frac{49}{2}^+)$	
624.9	5	−0.25(6)	−0.04(7)	$\frac{13}{2}^+ \rightarrow \frac{11}{2}^-$	$E1$
632.9	10	0.56(12)	−0.09(14)	$\frac{39}{2}^- \rightarrow \frac{35}{2}^-$	
637				$(\frac{23}{2}^- \rightarrow \frac{21}{2}^-)$	
638.1	18	0.27(4)	−0.07(5)	$\frac{33}{2}^- \rightarrow \frac{29}{2}^-$	$E2$
642.9	8	0.26(3)	0.02(4)	$(\frac{17}{2}^- \rightarrow \frac{15}{2}^-)$	$M1/E2$
668.4	16	0.48(7)	−0.32(9)	$\frac{51}{2}^- \rightarrow \frac{47}{2}^-$	$E2$
688.3	4			$(\frac{49}{2}^+ \rightarrow \frac{45}{2}^+)$	$(E2)$
692.2	2			$\frac{17}{2}^+ \rightarrow \frac{17}{2}^-$	
696.0	3	−0.18(30)	0.59(42)	$(\frac{53}{2}^- \rightarrow \frac{51}{2}^-)$	$(M1/E2)$
699.1	7	−0.94(11)	0.50(13)	$\frac{27}{2}^- \rightarrow \frac{25}{2}^-$	$M1/E2$
704.7	11	0.45(9)	−0.48(11)	$\frac{37}{2}^- \rightarrow \frac{33}{2}^-$	$E2$
709.8	39	−0.20(1)	−0.02(2)	$\frac{21}{2}^{(+)} \rightarrow \frac{19}{2}^-$	$E1$
731.5	19	0.31(1)	−0.13(1)	$\frac{19}{2}^- \rightarrow \frac{15}{2}^-$	$E2$
736.4	5	−0.41(8)	−0.05(10)	$(\frac{21}{2}^- \rightarrow \frac{17}{2}^-)$	
743.2	7			$\frac{41}{2}^- \rightarrow \frac{37}{2}^-$	
744.6	17			$\frac{43}{2}^- \rightarrow \frac{39}{2}^-$	
754.1	51	0.20(1)	−0.11(2)	$\frac{33}{2}^{(+)} \rightarrow \frac{29}{2}^{(+)}$	
760.3	5			$\frac{41}{2}^- \rightarrow \frac{37}{2}^-$	
766.4	28	0.60(3)	−0.24(4)	$\frac{39}{2}^{(+)} \rightarrow \frac{35}{2}^{(+)}$	
777	2			$(\frac{45}{2}^- \rightarrow \frac{41}{2}^-)$	
788.1	5	0.32(17)	−1.40(25)	$(\frac{53}{2}^-) \rightarrow (\frac{49}{2}^-)$	
790.6	5	0.34(8)	−0.09(11)	$\frac{23}{2}^- \rightarrow \frac{19}{2}^-$	$E2$
819.6	4			$(\frac{55}{2}^+ \rightarrow \frac{51}{2}^+)$	
840.3	14	0.06(7)	−0.09(9)	$\frac{39}{2}^{(+)} \rightarrow \frac{35}{2}^{(+)}$	$M1/E2$
881	3			$(\frac{57}{2}^- \rightarrow \frac{53}{2}^-)$	
895.1	7	0.37(8)	−0.21(10)	$\frac{43}{2}^- \rightarrow \frac{39}{2}^-$	$E2$

[a] The relative intensities are accurate to within ±5% for the strong lines.

($\alpha = \pm\frac{1}{2}$) of the $\pi h_{9/2}$ state; band 3 as the favored signature ($\alpha = +\frac{1}{2}$) of the $\pi i_{13/2}$ state; bands 4 and 5 as the 90-ns isomer band, and 6 and 7 as bands built on the $\pi h_{11/2}$ state.

B. The $\pi h_{9/2}$, $\pi i_{13/2}$-level systems

Evidence for the $\pi h_{9/2}$ band ($\frac{1}{2}^-[541]$) is best seen in the gates shown in Fig. 2. The strong 233.4–334.7–413.8–491.6–566.8-keV cascade exhausts much of the γ-ray intensity in ^{187}Au. Intensity variations, clearly seen in the 233.4 and 566.8-keV gates, suggest that there are other γ-ray transitions that feed into the $\pi h_{9/2}$ band at various levels. Some of these other transitions decay from band 2 which is believed to be the other signature ($\alpha = -\frac{1}{2}$) of the $\pi h_{9/2}$ band, and are seen clearly in Fig. 3. In addition to the members of the $\pi h_{9/2}$ band, the $\pi i_{13/2}$-band members are also observed in these coincidence gates.

The 259.4-keV γ ray observed in the gates shown in Fig. 3 is a member of the $\pi i_{13/2}$ band ($\frac{1}{2}^+[660]$), together

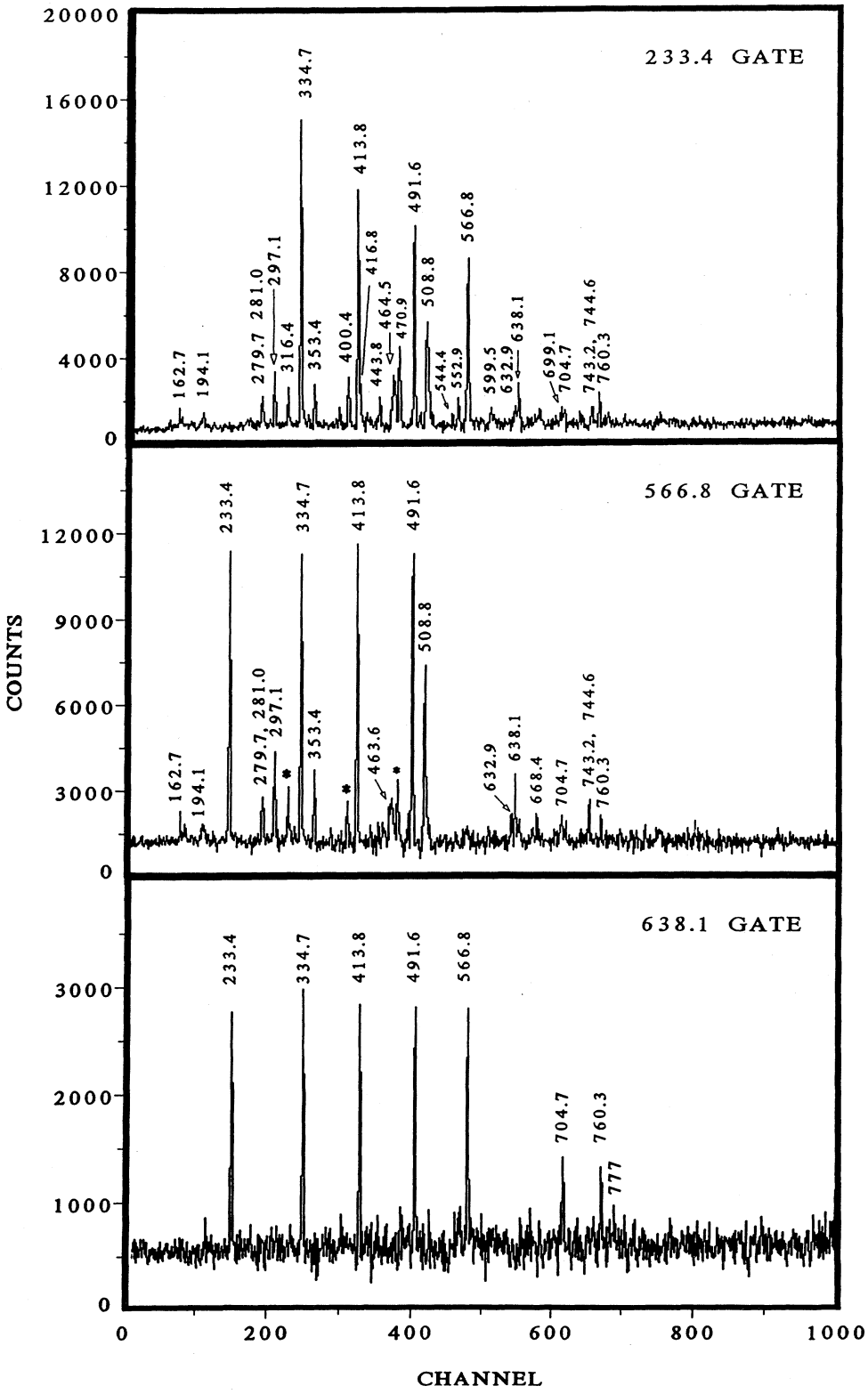

FIG. 2. Gamma-ray coincidence spectra for ^{187}Au gated on the 233.4-, 566.8-, and 638.1-keV transitions. Gamma-ray lines denoted by * in the 566.8-keV gate are those belonging to ^{186}Au.

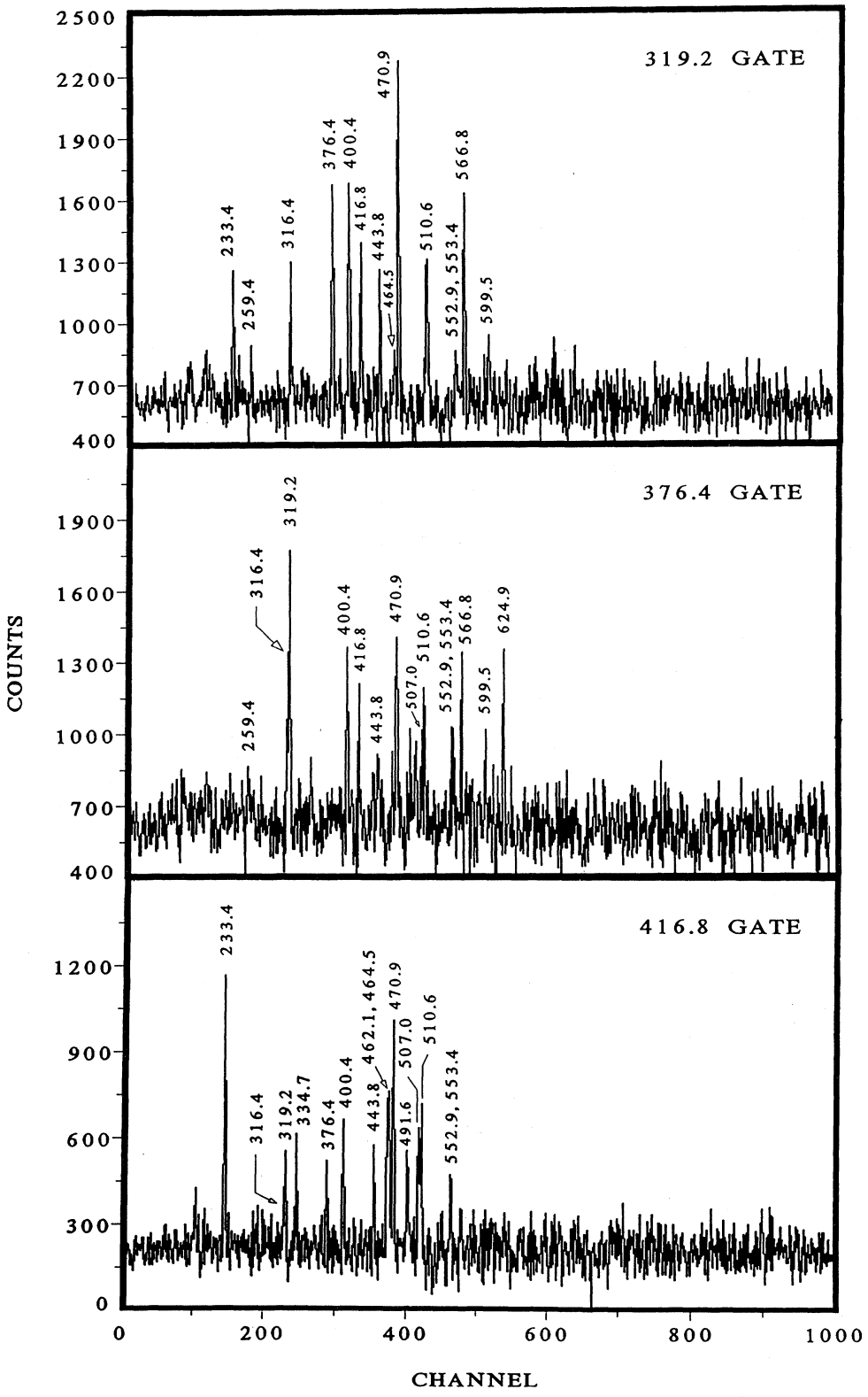

FIG. 3. Gamma-ray coincidence spectra for ^{187}Au gated on the 319.2-, 376.4-, and 416.8-keV transitions.

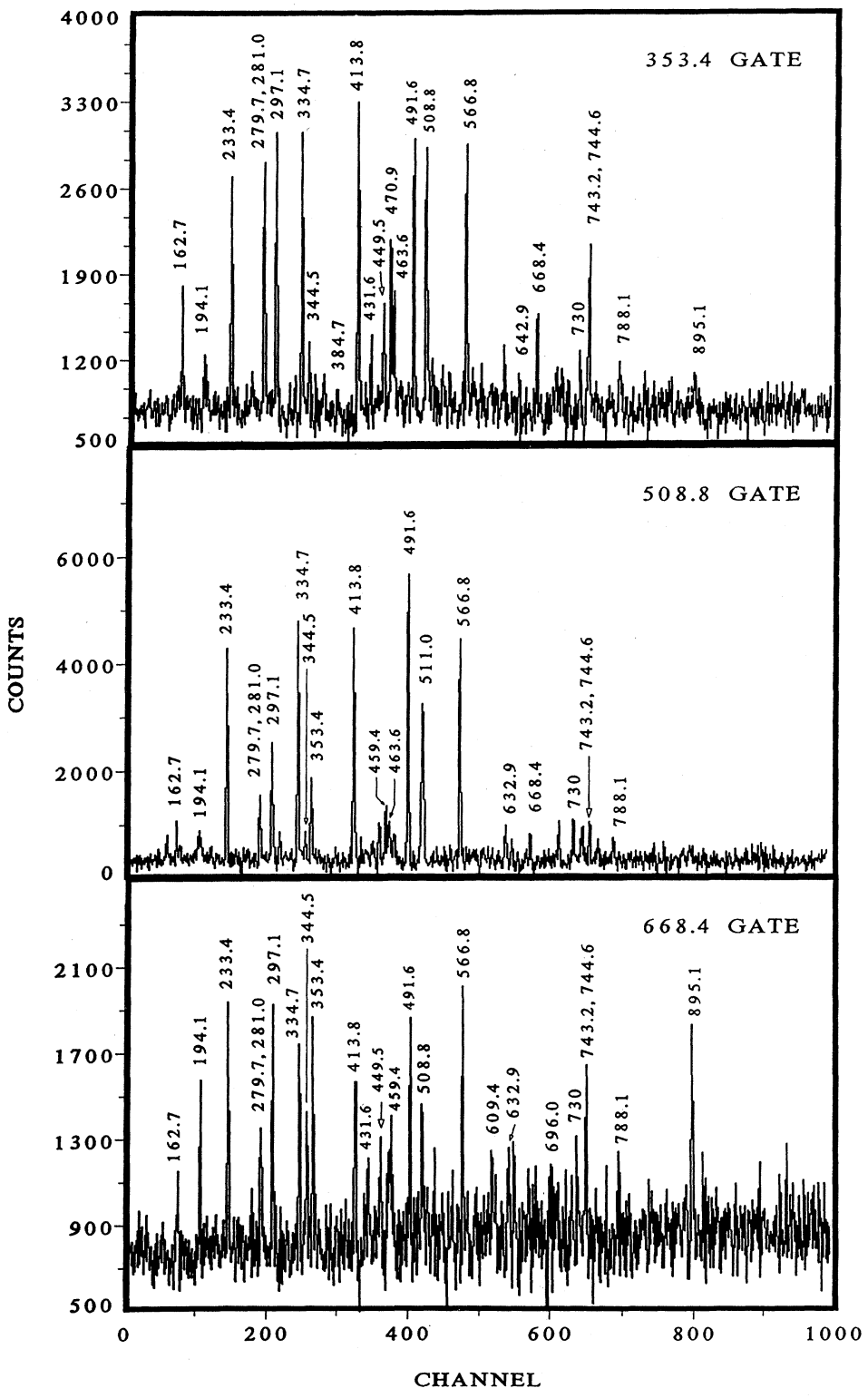

FIG. 4. Gamma-ray coincidence spectra for ^{187}Au gated on the 353.4-, 508.8-, and 668.4-keV transitions.

with the 316.4-, 400.4-, 470.9-, 443.8-, 510.6-, and the 599.5-keV transitions. The bandhead of this band had previously been located by Bourgeois *et al.*[7] and Wood *et al.*[16]

The measured angular distribution coefficients for the γ rays in the $\pi h_{9/2}$ band are characteristic of stretched $E2$ transitions. The $E2$ nature of the cascade of five transitions deexciting the $\frac{29}{2}^-$ level agrees with the results of earlier angular distribution measurements by Deleplanque *et al.*[6] The side-feeding members of band 1 (i.e., 376.4-, 544.4-, and 699.1-keV lines) all have angular distribution coefficients that are consistent with an $M1/E2$ assignment (see Table I). The 624.9-keV transition connecting the $\pi i_{13/2}$ band to the $\pi h_{9/2}$ ($\alpha=-\frac{1}{2}$) band has been assigned as a dipole transition based on the angular distribution measurements. The lack of transitions, from the 1122.0-keV level to the 120.7-keV level in the $\pi h_{9/2}$ band and from the 1381.4-keV level to the 354.1-keV level, supports the previous positive-parity assignment of the 1122.0-keV state.[16] The angular distribution coefficients for members of the $\pi i_{13/2}$ band resemble those of stretched $E2$ transitions.

C. The 90 ns isomer band

Some of the gamma rays seen in Fig. 2 to be in coincidence with the 233.4- and 566.7-keV lines were found to be actually in delayed coincidence. Gating on some of these lines allowed the isolation of a strongly coupled band, with an isomeric bandhead ($T_{1/2}=90\pm10$ ns) at 2669.8 keV, which decays primarily through a 508.8-keV transition. This isomeric decaying transition has been found to be of mixed $M1/E2$ character[17] which suggests that the bandhead has $J^\pi=\frac{31}{2}^-$. Evidence for this band is best seen in the γ-γ coincidence gates shown in Fig. 4 where the members of the $\pi h_{9/2}$ band below the 2161.0-keV level are seen to be in strong coincidence. The transitions that are higher up in the band are best seen in the 668.4-keV gate. All the gates in Fig. 4 display the members belonging to the 90-ns isomer band and a few of those belonging to the $\pi h_{9/2}$ and $\pi h_{11/2}$ bands. Therefore, in addition to the 508.8-keV transition which decays to the 2161.0-keV level of the $\pi h_{9/2}$ band, a weak 89-keV transition must also decay to the 2580.9-keV level of the $\pi h_{11/2}$ band. Although this γ transition has not been observed because of the presence of lead x rays, the total intensity of the 89-keV transition (including electron conversion) has been estimated from the coincidence data to be 21 units [$I_\gamma(89)=2$].

The 353.4-keV γ ray, one of the strongest members of this band, is also shown in Fig. 4 to provide evidence for the placement of some of the in-band γ-ray transitions. The 353.4-keV γ-ray transition is not in coincidence with the 516.0- and 632.9-keV transitions, suggesting that the 353.4-keV γ ray may be parallel to both of these. An unusual feature of this band is that there are two $\frac{43}{2}^-$ states, one at the 4506.7-keV level and the other at the 4657.2-keV level. Furthermore, no evidence of a $\frac{45}{2}^-$ state was observed. It is possible that the $\frac{49}{2}^-\rightarrow\frac{45}{2}^-$ decay is energetically unfavorable (with respect to the observed $\frac{49}{2}^-\rightarrow\frac{47}{2}^-$ decay) due to the expected large energy difference between the $\frac{41}{2}^-$ and $\frac{45}{2}^-$ states. This would result in a very small energy difference for the $\frac{49}{2}^-\rightarrow\frac{45}{2}^-$ decay which would mean that such a transition would have insufficient intensity to be observed.

D. The $\pi h_{11/2}$-level system

The construction of the $\pi h_{11/2}$ band was accomplished in the same manner as the other bands. The 449.5-keV γ-ray transition exhausts much of the γ-ray intensity. It is the lowest-lying member of the $\pi h_{11/2}$ band, and this agrees with the placement of Deleplanque *et al.*[6]

The measured $T_{1/2}=50\pm5$ ns for the $\frac{11}{2}^-$ state of the $\pi h_{11/2}$ band agrees with previous measurements.[6,7,18] Results from the isomer search experiment show that the 149.6-, 166.7-, 709.8-, 731.5-, and 449.5-keV transitions are delayed. This suggests that the level at 2431.7 keV is isomeric, and the lifetime analysis yields a $T_{1/2}=25\pm2$ ns. There is some doubt on the correct ordering of the 149.6- and 166.7-keV transitions, since the 149.6-keV γ ray is part of an unresolved doublet which makes it difficult to determine the relative positions of the 149.6- and 166.7-keV lines. (It was not possible to determine whether or not the 2282.1-keV level is also isomeric.)

IV. DISCUSSION

There are several features in ^{187}Au that are also observed in ^{181,183,185}Au.[8,13–15] Both signatures of the $\pi h_{9/2}$ band and the $\alpha=\frac{1}{2}$ signature of the $\pi i_{13/2}$ band have been assigned. Weak evidence of the $\pi f_{7/2}$ band is present (see below). These prolate structures have come down in energy from across the $Z=82$ closed shell. In addition, features of the heavier odd-A ^{189,191,193,195}Au (Refs. 19 and 20) isotopes were also seen in the ^{187}Au-level scheme. The $\pi h_{11/2}$ oblate structure was established up to spin $\frac{27}{2}^-$. A very extensive irregular structure built on $\frac{21}{2}^{(+)}$ and $\frac{25}{2}^{(+)}$ states was seen for the first time. A spin $\frac{31}{2}$ isomeric state was also observed and a strongly coupled band built on it has been established.

A. Prolate bands

A comparison of the aligned angular momenta[21] in the prolate bands can be used to determine the quasiparticle nature of both the bands and the aligning particles. In Fig. 5(a) the alignment, i, is plotted as a function of the rotational frequency, $\hbar\omega$. An initial alignment of about $5-6\hbar$ in the $\pi i_{13/2}$ band is consistent with that of an $i_{13/2}$ proton in a low-K orbital. The existence of this high initial alignment in band 3 presents further evidence that this band cannot be an $f_{7/2}$ band but the low-K $\pi i_{13/2}$ $\frac{1}{2}$[660] band instead. The $\pi i_{13/2}$ band is clearly seen to backbend at a rotational frequency of $\hbar\omega\simeq0.23$ MeV, with an alignment gain of 6.5 $\hbar$. The $\alpha=-\frac{1}{2}$ signature of the $\pi h_{9/2}$ band shows a kink in the alignment curve which is reminiscent of what was observed in ^{185}Au (Ref. 8). In that nucleus, a similar perturbing behavior was attributed to the interaction between the unfavored signa-

ture of the $\pi h_{9/2}$system and the favored $\pi f_{7/2}$ ($\alpha=-\frac{1}{2}$) band. The same description can be used to explain the perturbed behavior of the $\alpha=-\frac{1}{2}$ signature of the $\pi h_{9/2}$ band in ^{187}Au, even though the $\pi f_{7/2}$ band ($\frac{1}{2}^-[530]$) was not observed directly. The favored signature of the $\pi h_{9/2}$ band is observed to continue smoothly through the backbending region in the $\pi i_{13/2}$ band, and the start of an upbend is seen to occur at around $\hbar\omega \simeq 0.38$ MeV. In

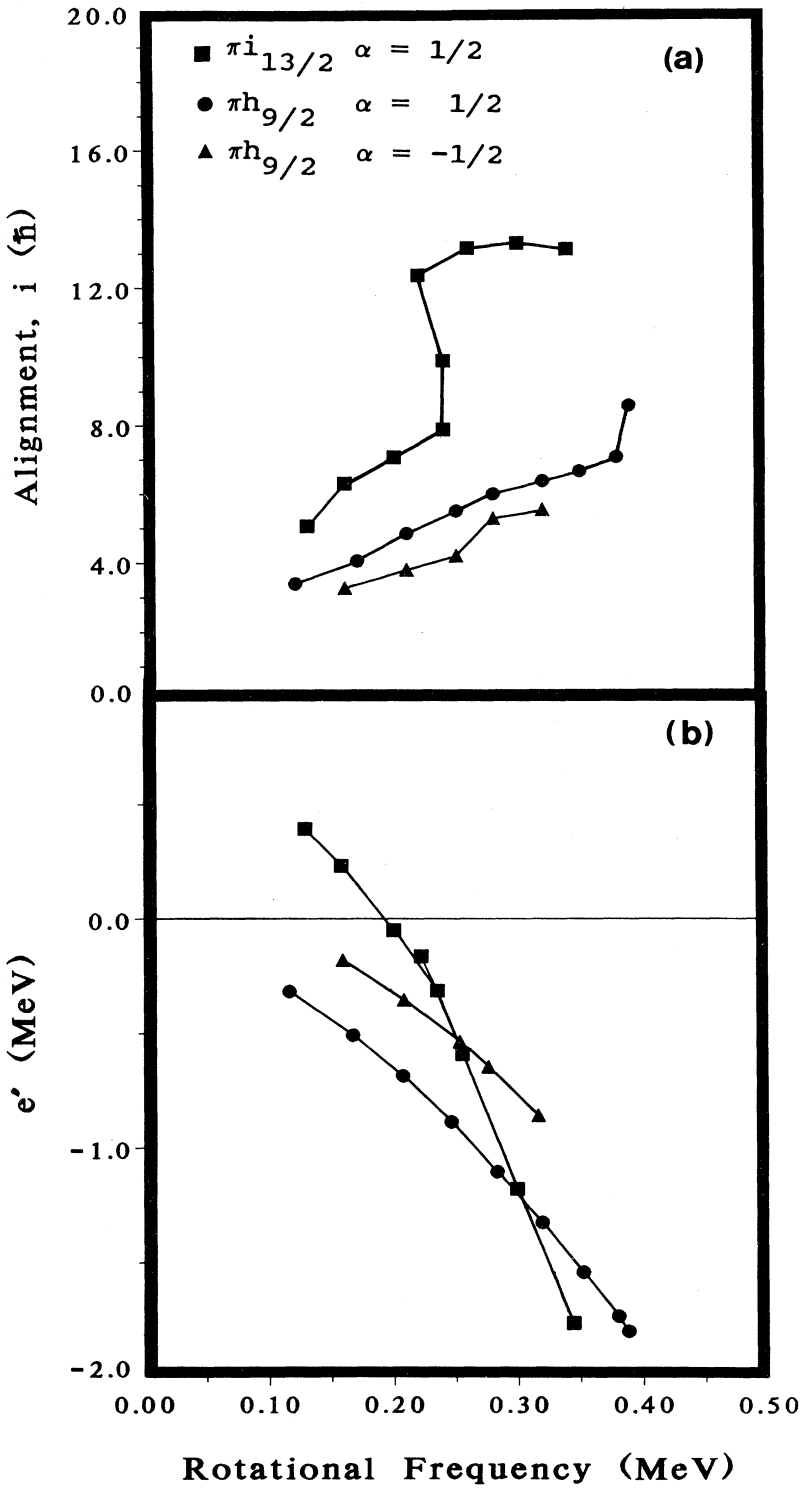

FIG. 5. Plots of the (a) alignment, i, and (b) experimental Routhians vs the rotational frequency for the prolate [$\pi i_{13/2}$ and $\pi h_{9/2}$ ($\alpha=\pm\frac{1}{2}$)] system. The calculations were based on $J_0=21$ MeV$^{-1}\hbar^2$ and $J_1=90$ MeV$^{-3}\hbar^4$.

^{185}Au, the $\pi h_{9/2}$ band is crossed at $\hbar\omega \simeq 0.32$ MeV with a total alignment gain of $\Delta i \simeq 5.7\hbar$. Larabee *et al.*[8] interpreted this crossing as the alignment of $i_{13/2}$ neutrons with the rotational axis.

In ^{184}Pt, it is argued[22] that the upbend ($\Delta i \simeq 9.7\hbar$) observed in the yrast band is a result of a four-quasiparticle alignment, two $h_{9/2}$ protons and two $i_{13/2}$ neutrons occurring at roughly the same rotational frequency ($\hbar\omega \simeq 0.25$ MeV). In ^{187}Au, there is no evidence of a $(\nu i_{13/2})^2$ alignment occurring at the above frequency, suggesting that the first neutron-band crossing has shifted towards higher rotational frequency. Since the $h_{9/2}$ orbital is blocked in the $\pi h_{9/2}$ band, the backbend seen in the $\pi i_{13/2}$ band is a result of a pair of $h_{9/2}$ protons aligning their angular momentum with the rotational axis. The upbend seen at a much higher frequency ($\hbar\omega \simeq 0.38$ MeV) in the $\pi h_{9/2}$ band may be due to the alignment of a pair of $i_{13/2}$ neutrons, analogous to the upbend ($\hbar\omega \simeq 0.4$ MeV) recently observed in the $\pi h_{9/2}$ band of the isotone ^{185}Ir.[23]

B. Oblate bands

The $\pi h_{11/2}$ band (labeled 6) is a result of the coupling of an $h_{11/2}$ proton-hole state to the ground-state band of the slightly deformed oblate Hg core. The $\pi h_{11/2}$ bands found in the odd-A ^{187,189,191,193}Au isotopes are all built on isomeric states. The $\pi h_{11/2}$ sequences in ^{189,191,193}Au display an alignment gain at spin $\frac{27}{2}^-$. Gono *et al.*[19] have interpreted the alignment in these bands as $\pi h_{11/2}$ holes coupled to a $(\pi h_{11/2})^2$ Hg core. However, Kölschbach *et al.*[20] have suggested that the alignment is a result of $\pi h_{11/2}$ holes coupling to $(\nu i_{13/2})^2$ Hg cores.

Similar features can be seen in the $\pi h_{11/2}$ band in ^{187}Au, where there is a significant increase in alignment during the transition from band 6 to bands 4 and 5. The intensity of the 384.7-keV transition was too weak to allow a determination of whether or not the $\frac{27}{2}^-$ state is isomeric as it is in ^{189,191,193}Au. Figure 6 shows a comparison of odd-odd ^{186,188}Au 11^- bands and the strongly coupled band of ^{187}Au. The data for ^{186,188}Au are from Janzen *et al.*[24] and similar structures have been observed in ^{190,192,194}Au by Neskakis *et al.*[25] They have interpreted these bands as having a $(\pi h_{11/2})(\nu i_{13/2})$ two-quasiparticle configuration coupled to the slightly oblate Hg cores. The three bands shown in Fig. 6 display very similar structures which suggests that the $\frac{31}{2}^-$ isomeric band found in ^{187}Au can be explained in terms of the 11^- $(\pi h_{11/2})$ $(\nu i_{13/2})$ bands in the heavier odd-odd Au isotopes. The most likely configuration for the bandhead is a $\frac{31}{2}^-$ $(\pi h_{11/2})\otimes(\nu i_{13/2})^2$ 10^+. The corresponding $(\nu i_{13/2})^2$ 10^+ configuration has been located in ^{188}Hg (Ref. 11) at an excitation energy of 2661 keV. This may be compared with an energy difference of 2445 keV for the $\frac{31}{2}^-$ and $\frac{11}{2}^-$ states. A consistent explanation of bands 4, 5, and 6 arises by comparing alignments for the $\frac{31}{2}^-$ band with that for the yrast band in ^{188}Hg. Figure 7 shows this comparison where the lowest excitations of the $h_{11/2}$ ($\alpha = \pm\frac{1}{2}$) sequences are also included. The alignment gain at the backbend in ^{188}Hg is $\simeq 11\hbar$ and in ^{187}Au, it is $\simeq 11\hbar$ as well. It is clear that this entire decay sequence in ^{187}Au results from coupling an $h_{11/2}$ hole

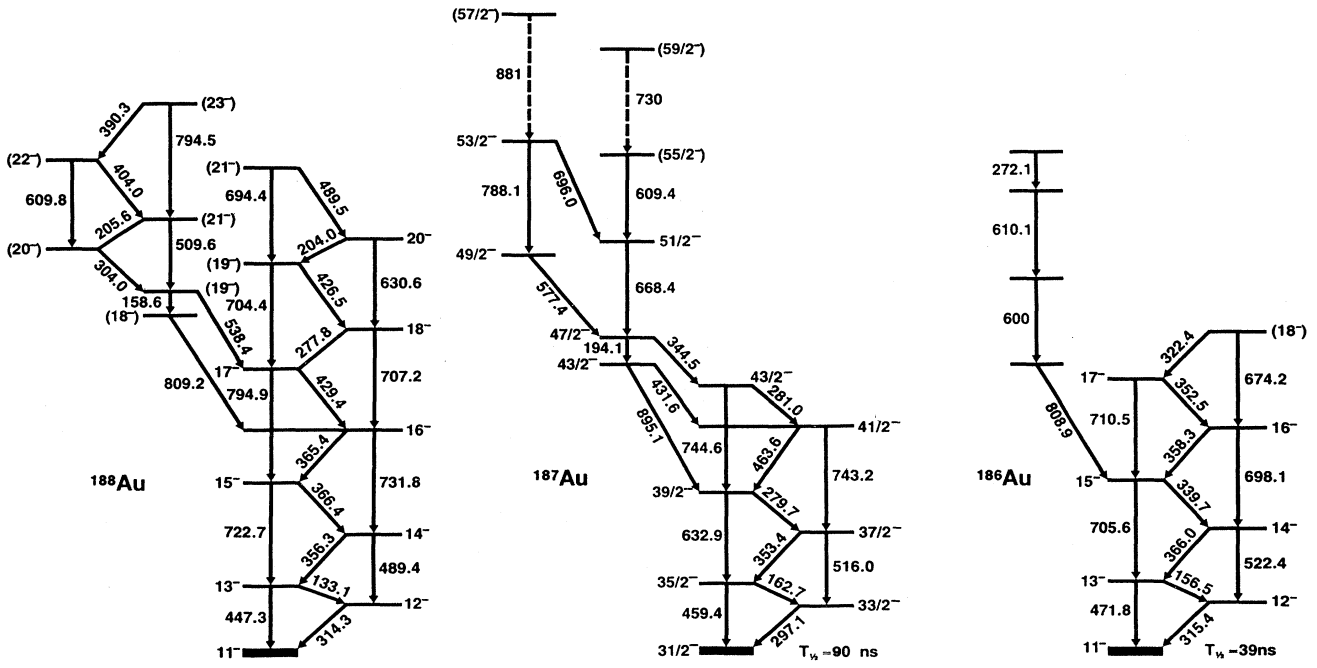

FIG. 6. Level schemes for the 11^- bands in ^{186,188}Au and the $\frac{31}{2}^-$ isomer band in ^{187}Au. The data for ^{186,188}Au are from Janzen *et al.*[24]

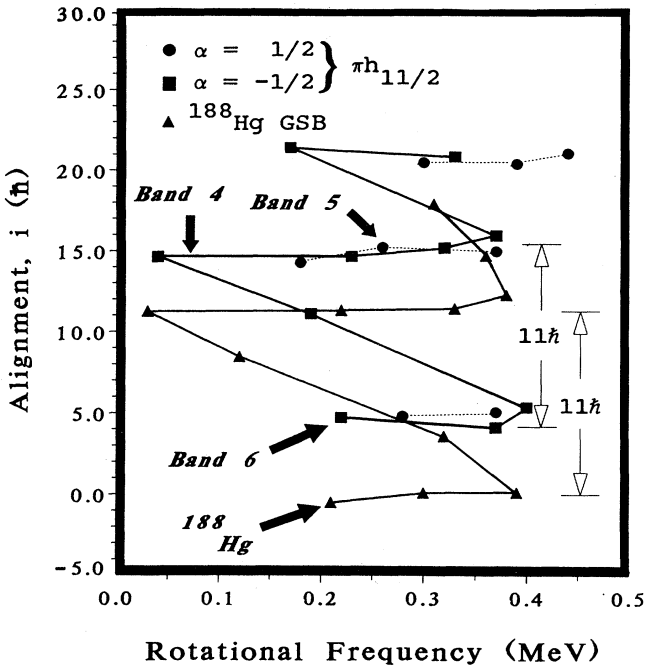

FIG. 7. Plots of the alignment i vs the rotational frequency for bands 4, 5, and 6 compared with the yrast sequence in ^{188}Hg. The calculations were based on $J_0=8$ MeV$^{-1}\hbar^2$ and $J_1=40$ MeV$^{-3}\hbar^4$.[11]

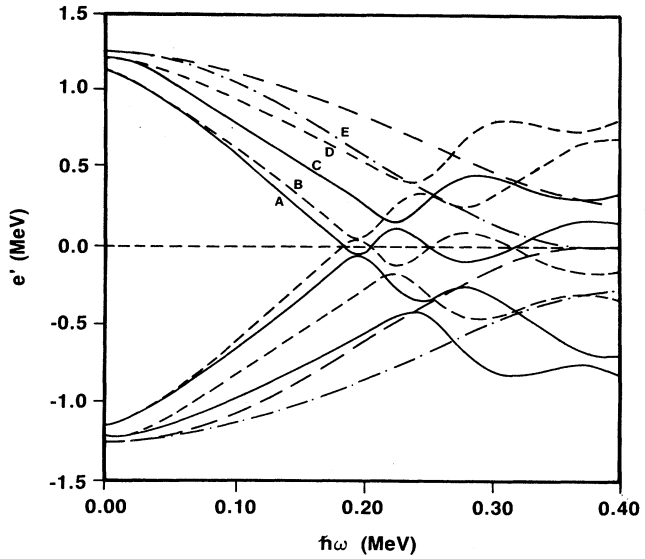

FIG. 8. Woods-Saxon cranked shell-model Routhians for neutrons for the $N=108$ nucleus ^{187}Au. Pairing values result from a self-consistent BCS calculation at $\omega=0$, with a reasonable decrease as a function of rotational frequency. The parameters used were $\beta_2=0.180$, $\beta_4=0.000$, and $\gamma=-60°$. The following notation is used. Full lines (——) are used for quasiparticle trajectories with positive parity and signature $\alpha=\frac{1}{2}$, that is $(+,+\frac{1}{2})$; short-dashed (— — —) lines for $(+,-\frac{1}{2})$; dot-dashed (—·—·—·) lines for $(-,+\frac{1}{2})$; and long-dashed (— — — —) lines for $(-,-\frac{1}{2})$.

which has an initial alignment of about four units to the ^{188}Hg core.

The 89-keV $E2$ transition is very slow (approximately 0.5 Weisskopf units), presumably because the backbend is so sharp that the R quantum number is good and has to be changed by 10 or 12 units.

Total Routhian surface (TRS) calculations[26] suggest that the $\pi h_{11/2}$ configuration in ^{187}Au would have a deformation of $\beta_2\simeq 0.18$ and a $\gamma\simeq -60°$. This is consistent with an $h_{11/2}$ hole coupled to the ^{188}Hg core, which has been interpreted as having a very similar deformation.[11] The fact that both signatures are seen in the odd proton nucleus allows conclusions to be made concerning the gamma deformation by comparing the observed signature splitting with that predicted by the cranked shell model (CSM). The quasiparticle neutron spectrum represented in Fig. 8 shows that a sharp backbend should occur at $\hbar\omega\simeq 0.21$ MeV due to the alignment of a pair of $\nu i_{13/2}$ quasiparticles. Experimentally, a Δi of $11\hbar$ is found at a crossing frequency of 0.25 MeV. Our TRS calculations indicate that this $i_{13/2}$ alignment should drive the gamma deformation from about $-74°$ to $-59°$. This should considerably reduce the signature splitting as seen in Fig. 9. This is seen to be the case experimentally where $\Delta e'$ changes from 350 to 75 keV at $\hbar\omega\simeq 0.22$ MeV.

Figure 7 reveals that a second backbend in ^{188}Hg is also mirrored in ^{187}Au. This backbend could result from the alignment of a second pair of $i_{13/2}$ neutrons or from a pair of $h_{9/2}$ protons. The cranked shell model favors the former situation with the proton crossing not expected until $\hbar\omega\simeq 0.40$ MeV. As expected, the alignment gain at this CD crossing is less than for the AB crossing and the interaction is larger. The increase in signature splitting after this second backbend indicates that the gamma deformation has become more negative again.

The structure labeled 7 in Fig. 1 decays into the oblate

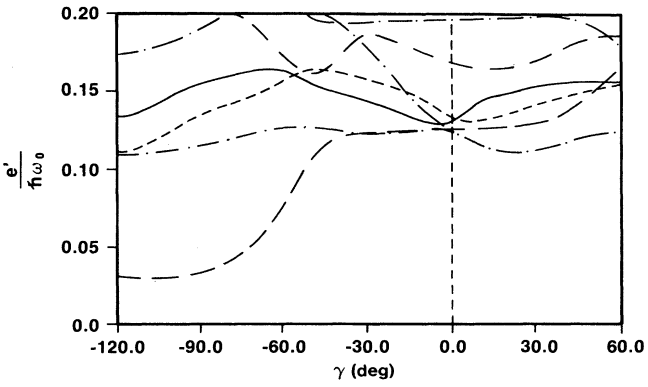

FIG. 9. Theoretical quasineutron Routhians e' (MeV) vs gamma deformation for the $\pi h_{11/2}$ band in ^{187}Au. Calculations were performed with the parameters $\beta_2=0.180$, $\beta_4=0.000$ at $\omega=0.03\omega_0=0.22$ MeV/$\hbar$. Refer to the caption of Fig. 8 for an explanation of the notation.

$\pi h_{11/2}$ band via the 709.8-keV transition. In ^{185}Au (Ref. 8) a strongly coupled band was found to decay into the decoupled band. The difference between ^{185}Au and ^{187}Au indicates that the oblate minimum is deeper in ^{187}Au than in ^{185}Au. The sequence seen in ^{187}Au is characteristic of a system that is continually changing its configuration. The $\frac{21}{2}^{(+)}$ and $\frac{25}{2}^{(+)}$ states observed in this band are similar to those in ^{189,191,193,195}Au. The $\frac{21}{2}^{+}$ states found in ^{189,191,193,195}Au have been interpreted as the coupling of an $h_{11/2}$ proton hole to the 5^- states in the Hg isotopes.[19,27] In ^{191,193}Au the $\frac{25}{2}^{+}$ states were identified as the coupling of an $h_{11/2}$ proton hole to the 7^- states in the Hg cores.[19] The $\frac{21}{2}^{(+)}$, $\frac{23}{2}^{(+)}$, and $\frac{25}{2}^{(+)}$ levels observed in ^{187}Au in the present work have similar excitation energies relative to the $\frac{11}{2}^{-}$ state as the 5^-, 6^-, and 7^- levels in ^{188}Hg have relative to the ground state.[11] Thus it appears that these states are formed by coupling the $h_{11/2}$ hole to these oblate Hg core states.

V. CONCLUSION

The study of the odd-mass ^{187}Au nucleus has provided excellent results on a variety of types of nuclear structure. Shape coexistence was observed beginning at low-excitation energies and surviving up to relatively high-spin states. Decoupled prolate bands were found built on the $\pi h_{9/2}$ and $\pi i_{13/2}$ particle states which extend up to spins $\frac{45}{2}^{-}$ and $\frac{49}{2}^{+}$ respectively. These bands are consistent with the same configurations found in ^{185}Au. A strongly coupled oblate structure built on a $\frac{31}{2}^{-}$ isomeric state was observed for the first time. In addition, structures based on the $h_{11/2}$ proton-hole state were seen to much higher spin values than were previously known. The irregular spacing of the excitation energy levels in the $\pi h_{11/2}$ system is characteristic of oblate shaped nuclei.

The presence of prolate and oblate structures in ^{187}Au is in agreement with what is expected to occur in the Pt-Au-Hg region. The $\pi h_{11/2}$ system presents a good example of the coupling of a proton $h_{11/2}$ hole to the slightly deformed oblate ground state of the even-even Hg core. The $\frac{31}{2}^{-}$ isomer structure is comparable to the 11^- states in the heavier odd-odd Au isotopes, and the $\frac{21}{2}^{(+)}$, $\frac{23}{2}^{(+)}$, and $\frac{25}{2}^{(+)}$ levels correspond to the 5^-, 6^-, and 7^- states in the even-even Hg isotopes. On the other hand, the $h_{9/2}$ and $i_{13/2}$ bands show coupling of the respective protons to the prolate even-even Pt cores. Such systematic comparisons have been proven to be necessary and helpful in determining band configurations and the validity of the CSM in this region.

ACKNOWLEDGMENTS

The McMaster University Tandem Accelerator Laboratory operates under a grant from the Canadian Natural Sciences and Engineering Research Council. Research at the University of Tennessee is supported by the U.S. Department of Energy under Contract No. DE-SG05-40361.

---

*Present address: Department of Nuclear Physics, Research School of Physical Sciences, Australian National University, Canberra, ACT 2601, Australia.

†Present address: The Niels Bohr Institute, Risø, DK-4000 Roskilde, Denmark.

‡Present address: Chalk River Nuclear Laboratories, Atomic Energy of Canada Limited, Chalk River, Ontario, Canada K0J 1J0.

§Present address: TRIUMF, Vancouver, British Columbia, Canada V6T 2A3.

**Present address: Lanzhou University, Lanzhou, People's Republic of China.

[1]J. Bonn, G. Huber, and H. J. Kluge, U. Köpf, L. Kugler, and E. W. Otten, Phys. Lett. **36B**, 41 (1971).

[2]N. Rud, D. Ward, H. R. Andrews, R. L. Graham, and J. S. Geiger, Phys. Rev. Lett. **31**, 1421 (1974).

[3]D. Proetel, R. M. Diamond, and F. S. Stephens, Nucl. Phys. **A231**, 301 (1974).

[4]R. M. Leider, H. Benscher, W. F. Davidson, A. Neskakis, and C. Mayer-Böricke, Nucl. Phys. **A248**, 317 (1975).

[5]M. Guttormsen, Y. K. Agarwal, C. Günther, K. Hardt, H. Hübel, A. Kalbus, R. Kroth, G. Mikus, J. Recht, and P. Schüler, Nucl. Phys. **A383**, 541 (1982).

[6]M. A. Deleplanque, C. Gerschel, M. Ishihara, C. Bourgeois, M. G. Desthuilliers, N. Perrin, J. P. Husson, P. Kilcher, J. Letessier, and V. Berg, J. Phys. (Paris) **36**, L-205 (1975).

[7]C. Bourgeois, P. Kilcher, J. Lettessier, V. Berg, and M. G. Desthuilliers, Nucl. Phys. **A295**, 424 (1978); C. Bourgeois (private communication).

[8]A. J. Larabee, M. P. Carpenter, L. L. Riedinger, L. H. Courtney, J. C. Waddington, V. P. Janzen, W. Nazarewicz, J-Y. Zhang, R. Bengtsson, and G. A. Leander, Phys. Lett. **169B**, 21 (1986).

[9]G. Hebbinghaus, W. Gast, A. Kramer-Flecken, R. M. Lieder, J. Skalski, and W. Z. Urban, Nucl. Phys. **A328**, 387 (1987).

[10]S. Pilotte, Ph.D. thesis, Université de Montréal, 1987; S. Pilotte *et al.* (unpublished).

[11]F. Hannachi, G. Bastin, M. G. Porquet, C. Schuck, J. P. Thibaud, C. Bourgeois, L. Hildingsson, D. Jerrestam, N. Perrin, H. Sergolle, F. A. Beck, T. Byrski, and J. C. Merdinger, Nucl. Phys. **A481**, 135 (1988).

[12]G. P. Palameta and J. C. Waddington, Nucl. Instrum. Methods **A234**, 476 (1985).

[13]H. Q. Jin, M. P. Carpenter, V. P. Janzen, L. L. Riedinger, L. Zhou, C. Baktash, M. L. Halbert, N. R. Johnson, I. Y. Lee, F. K. McGowan, and M. A. Riley, University of Tennessee Progress Report on Nuclear Spectroscopy Studies, Document No. 88-03, 1988 (unpublished).

[14]M. P. Carpenter, V. P. Janzen, C. R. Bingham, A. J. Larabee, L. L. Riedinger, W. Schmitz, C. Baktash, M. L. Halbert, N. R. Johnson, I. Y. Lee, M. N. Rao, J. Nyberg, and C. D. Papanicolopoulous, University of Tennessee Progress Report on Nuclear Spectroscopy Studies, Document No. 87-01, 1987 (unpublished); Bull. Am. Phys. Soc. **31**, 874 (1986).

[15]L. Zhou, M. P. Carpenter, C. R. Bingham, L. H. Courtney, V. P. Janzen, H. Q. Jin, W. Schmitz, C. Baktash, M. L. Halbert,

N. R. Johnson, I. Y. Lee, M. N. Rao, J. Nyberg, and C. D. Papanicolopoulous, University of Tennessee Progress Report on Nuclear Spectroscopy Studies, Document No. 88-03, 1988 (unpublished).

[16]J. L. Wood (private communication); C. D. Papanicolopoulous, M. A. Grimm, J. L. Wood, E. F. Zganjar, M. O. Kortelahti, J. D. Cole, and H. K. Carter, Z. Phys. A **330**, 371 (1988).

[17]Ch. Vieu, J. S. Dionisio, J. M. Lagrange, M. Pautrat, and J. Vanhorenbeek, Instituto Politécnico Nacional Annual Report No. IPN 38, 1986.

[18]V. Berg, Z. Hu, J. Oms, and C. Ekström, Nucl. Phys. **A410**, 445 (1983).

[19]Y. Gono, R. M. Lieder, M. Müller-Veggian, A. Neskakis, and C. Mayer-Böricke, Nucl. Phys. **A327**, 269 (1979).

[20]V. Kölschbach, P. Schüller, D. Hardt, C. Rosendaal, C. Gunther, K. Euler, M. Tölle, M. Marten-Tölle, and P. Zeyen, Nucl. Phys. **A439**, 189 (1985).

[21]R. Bengtsson and S. Frauendorf, Nucl. Phys. **A327**, 139 (1979).

[22]M. P. Carpenter, Ph.D. thesis, University of Tennessee, 1988; M. P. Carpenter *et al.* (unpublished).

[23]D. L. Balabanski, G. Hebbinghaus, R. M. Lieder, W. Gast, A. Krämer-Flecken, T. Morek, T. Rzaca-Urban, and W. Urban, Kernforschungsanlage Jülich GmbH, Institut für Kernphysik, Annual Report No. 35, 1987 (unpublished).

[24]V. P. Janzen, Z.-M. Liu, M. P. Carpenter, L. H. Courtney, A. J. Larabee, L. L. Riedinger, J. K. Johansson, D. G. Popescu, and J. C. Waddington, Bull. Am. Phys. Soc. **31**, 1235 (1986).

[25]A. Neskakis, R. M. Lieder, H. Beuscher, Y. Gono, D. R. Haenni, and M. Müller-Veggian, Phys. Lett. **80B**, 194 (1979); Nucl. Phys. **A390**, 53 (1982).

[26]W. Nazarewicz *et al.*, Oak Ridge National Laboratory Physics Division Progress Report No. 85, 1986 (unpublished); W. Nazarewicz *et al.* (unpublished).

[27]P. O. Tjøm, M. R. Maier, D. Benson, Jr., F. S. Stephens, and R. M. Diamond, Nucl. Phys. **A231**, 397 (1974).